Protist, Vol. 158, 193—207, April 2007
http://www.elsevier.de/protis
Available online 7 December 2006

Protist

ORIGINAL PAPER

Reproductive Isolation among Sympatric Cryptic Species in Marine Diatoms

Alberto Amato[a,1], Wiebe H.C.F. Kooistra[a], Jung Hee Levialdi Ghiron[a], David G. Mann[b], Thomas Pröschold[c], and Marina Montresor[a]

[a]Stazione Zoologica 'A. Dohrn', Villa Comunale, 80121 Napoli, Italy
[b]Royal Botanic Garden, Edinburgh EH3 5LR, Scotland, UK
[c]Culture Collection of Algae and Protozoa, Scottish Association for Marine Science, Dunstaffnage Marine Laboratory, Dunbeg by Oban, Argyll PA37 1QA, Scotland, UK

Submitted August 18, 2006; Accepted October 1, 2006
Monitoring Editor: Robert A. Andersen

Pseudo-nitzschia **is a marine cosmopolitan genus of chain-forming planktonic diatoms. As for the vast majority of phytoplankton organisms, species identification within this genus mostly relies upon morphological features. Taxa were initially identified based on cell shape and gross morphology of their composite silica cell wall, called the frustule. Yet, observations of the frustule in electron microscopy showed many additional characters for species identification and results of molecular studies have demonstrated that genetically distinct groups might exist within morpho-species. However, these studies have not addressed the biological meaning of these genetic differences. Here, we bridge that gap by comparing ultrastructural features and sequence data (three ribosomal and one plastid marker) of 95 strains with results of mating experiments among these strains. Experiments were performed on two morphologically distinct entities:** ***P. delicatissima*** **and** ***P. pseudodelicatissima*****. Each of the two entities consisted of multiple genetically distinct and reproductively isolated taxa, all occurring in sympatry:** ***P. delicatissima*** **was composed of three phylogenetic and reproductively distinct groups, whereas** ***P. pseudodelicatissima*** **consisted of up to five. Once these taxa had been defined both genetically and biologically, subtle ultrastructural differences could be detected as well. Our findings not only show that cryptic genetic variants abound in sympatry, but also that they are reproductively isolated and, therefore, biologically distinct units.**

Key words: diatoms; cryptic diversity; *Pseudo-nitzschia*; reproductive isolation; species concept.

Introduction

Species are fundamental natural units (Coyne and Orr 2004) and their proper circumscription is an essential requirement for both biodiversity assessments and a correct understanding of their ecology, biogeography, evolutionary history, and speciation mechanisms. Within the unicellular eukaryote plankton, biodiversity estimates are still based mainly on morphological features but results of recent molecular taxonomic assessments suggest that phytoplankton biodiversity is seriously underestimated. For instance, entirely new lineages are being found (Guillou et al. 2004; Massana et al. 2004) as well as genetically distinct entities within morphologically delineated species

[1]Corresponding author;
fax +39 081 7641355
e-mail amato@szn.it (A. Amato).

doi:10.1016/j.protis.2006.10.001

(Montresor et al. 2003; Sáez et al. 2003; Sarno et al. 2005). Cryptic and pseudo-cryptic species thus exist in phytoplankton, just as in other plant and animal groups (Knowlton 1993; Sáez and Lozano 2005). They are difficult or impossible to distinguish based on morphological characters, but hide divergence in habitat, physiology, or life cycle traits, with obvious ecological implications.

In the present study, we compare morphological and genetic species circumscriptions with mating delineation in sympatric populations of the planktonic diatom genus *Pseudo-nitzschia*. This genus is an important constituent of coastal and oceanic phytoplankton blooms and some of its species are notorious for producing domoic acid, a neurotoxin responsible for Amnesic Shellfish Poisoning (ASP; Mos 2001). The needle-shaped cells form stepped chains by cells holding on to one another at their apices (Fig. 1A,B). Subtle morphological differences in cell shape and size and in the overlapping patterns of cell apices in the chain represent the only characters for identifying *Pseudo-nitzschia* species by light microscopy (LM). Detailed examination of their compound silica cell wall, called the frustule, using electron microscopy (Fig. 1C,D), is generally necessary for accurate species identification (Hasle and Syvertsen 1997).

The frustule is composed of two valves and accompanying sets of girdle bands. In *Pseudo-nitzschia*, each valve possesses a slit, called the raphe, which runs along the whole length of the valve and is reinforced on the interior side with silica bridges, called fibulae (Fig. 1C,D; dotted arrows). In some species (including those treated here), the raphe slit is interrupted centrally by a small thickened nodule and the fibulae on either side of this nodule are more widely spaced (Fig. 1C,D; solid arrows). The valve is ornamented with striae (Fig. 1C,D; solid ellipses) — weakly silicified strips containing small poroids (Fig. 1C,D; arrowheads) — alternating with more heavily silicified, rib-like strips, called interstriae (Fig. 1C,D; dotted ellipses). The poroids may be subdivided by sets of struts (cribra, Fig. 1C) resembling the tracery of stained glass windows and they are also occluded by thin, porous silica sheets (hymens).

Morphological investigations by Hasle (Hasle 1965; Hasle and Syvertsen 1997) showed considerable diversity in valve structure and ornamentation and led to the description of around 20 species. These included *P. delicatissima* and *P. pseudodelicatissima*, called *Nitzschia actydrophila* and *N. delicatula* by Hasle (1965), which, although having similarly short overlaps between cells in chains, could be separated by cell shape using LM: *P. delicatissima* cells have truncated ends in girdle view, whereas *P. pseudodelicatissima* cells have pointed ends and their valves are more linear, with a sharper differentiation of the

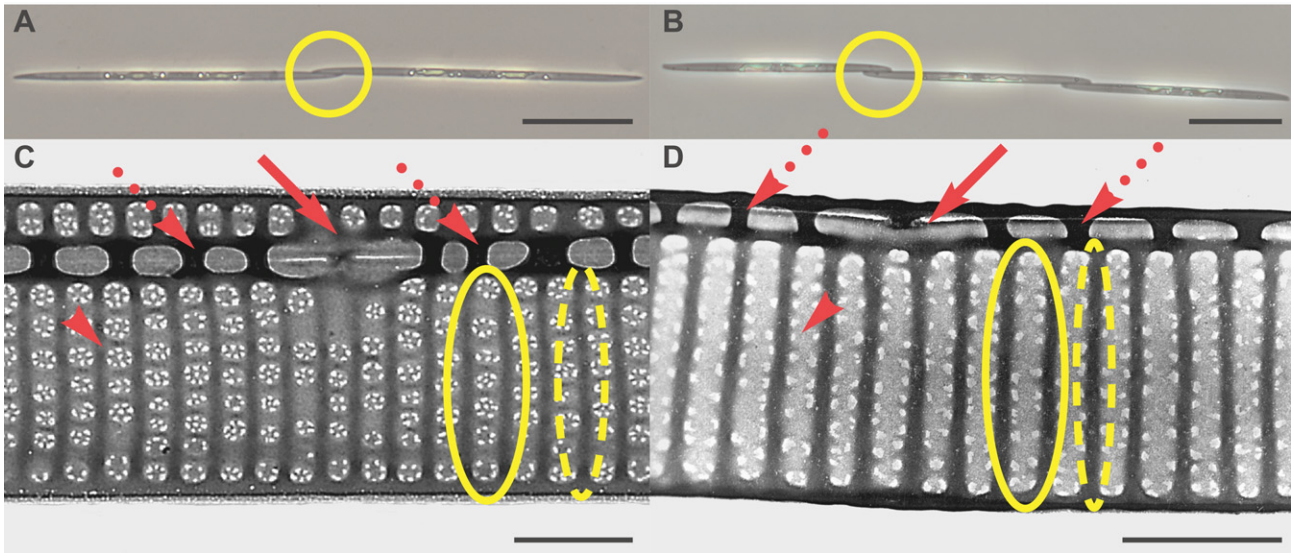

Figure 1. Micrographs from light **(A,B)** and transmission electron microscopy **(C,D)** of *Pseudo-nitzschia calliantha* pse4 **(A—C)** and *Pseudo-nitzschia delicatissima* del1 **(B—D)**. Solid circles indicate the overlapping region between two adjacent cells in a chain, dotted arrows the fibulae, solid arrows the wider separation of the two central fibulae, solid ellipses the striae, dotted ellipses the interstriae, and arrowheads the poroids. Scale bars: 20 μm **(A,B)**, 1 μm **(C,D)**.

overlapping region (Fig. 1B vs. 1A) (Hasle and Syvertsen 1997). Both species have recently been investigated using molecular genetic methods and found to be heterogeneous, leading to revision of existing species and description of new species, based on sequence data and subtle ultrastructural differences (Lundholm et al. 2003, 2006).

Sexual reproduction can be obtained in laboratory conditions for some *Pseudo-nitzschia* species (Amato et al. 2005; Davidovich and Bates 1998) and they are thus amenable for testing the biological species concept, i.e. whether the different taxa represent reproductively isolated units. Like most diatoms, *Pseudo-nitzschia* has a diplontic life cycle consisting of a prolonged period of mitotic divisions and a brief sexual phase. Due to the peculiar mode of division in diatoms, in which the newly formed daughter valve is synthesized within the parent cell, the average cell size of a population gradually decreases with time. For most diatoms, including *Pseudo-nitzschia*, sexual reproduction is the only way out of this miniaturization trap, and involves meiosis, gamete fusion, and the formation of a specialized zygote, called auxospore, which expands and produces a cell of maximum size (Chepurnov et al. 2004), called the initial cell. Almost all *Pseudo-nitzschia* species have a heterothallic (dioecious) mating system — i.e. meiosis is induced only when strains of the opposite mating type are brought together — and this greatly facilitates experimental design (Amato et al. 2005). The only known exception is *P. subcurvata*, reported as *Nitzschia subcurvata* (Fryxell et al. 1991), in which auxospores were observed in a monoclonal culture.

In the present study, we assess whether sympatric, genetically distinct, but morphologically extremely similar entities within *Pseudo-nitzschia* are reproductively isolated. We sampled 95 strains from our study area, the Gulf of Naples (Italy, Mediterranean Sea) that had *P. delicatissima*-like ('del') or *P. pseudodelicatissima*-like ('pse') morphologies when examined by LM. Strains were classified accordingly as 'del' or 'pse', respectively. No attempt was made initially to allocate clones of any of the species described within the *delicatissima* or *pseudodelicatissima* groups (Lundholm et al. 2003, 2006). Our goals were (1) to identify genetically distinct groups of strains utilizing four molecular markers, (2) to test mating compatibility within and among genetically circumscribed groups of strains, and (3) to search for ultrastructural differences among the frustules of the different groups.

Results

Genetic Diversity

Molecular analyses were carried out using the hypervariable domains D1—D3 of the 28S rDNA (LSU), the internal transcribed spacers (ITS-1 and ITS-2) of rDNA, and the plastid gene that encodes for the large subunit of RuBisCo (*rbc*L). For *rbc*L, 71% of the base changes were observed in the 3rd, 22% in 1st, and 7% in 2nd codon position. Results of genotype and haplotype groupings among the strains are depicted in Figure 2. The colour markings of the groups are based on the ITS-2 genotypes and are provided to guide the reader. Genotype groups observed in the nuclear rDNA sequences (Fig. 2B—D) corroborated the haplotype groupings observed in the *rbc*L (Fig. 2A) sequences except in three cases. First, within the *P. delicatissima*-like strains of del1 (blue), the plastid gene sequence showed two haplotypes, which differed by four substitutions, whereas nuclear markers recovered only single genotypes. Second, within the *P. pseudodelicatissima*-like strains of pse1 (red) and pse2 (yellow), *rbc*L and ITS-2 sequences identified two clades, but the strains shared identical LSU sequences. Moreover, ITS-1 further separated pse1 (red) into two sub-clades. The third mismatch was found among *P. pseudodelicatissima*-like strains pse3 (orange) and pse4 (dark brown). The anomaly was strain AL-112 that possessed *rbc*L haplotype pse3, but had nuclear genotypes typical for pse4 strains. This finding was confirmed by repeating PCR amplification and sequencing of both gene regions on two different DNA extractions from this strain.

Morphological Diversity

Examination of the frustule ultrastructure (Table 1) revealed differences among both *P. delicatissima*-like and *P. pseudodelicatissima*-like strains. Groups defined by ultrastructural details corroborated groups delineated by ITS-2 sequences (Fig. 2A). The *P. delicatissima*-like strains grouped into three distinct groups. In one of them (del1, blue), valve ultrastructure conformed to the description of *P. delicatissima sensu stricto* (Lundholm et al. 2006) and another one (del3, violet) could be identified as *P. dolorosa* (Lundholm et al. 2006). The third morphological group (del2, green) did not match any described *Pseudo-nitzschia* species. Cells were similar to *P. delicatissima* in terms of valve outline, ornamentation, and the

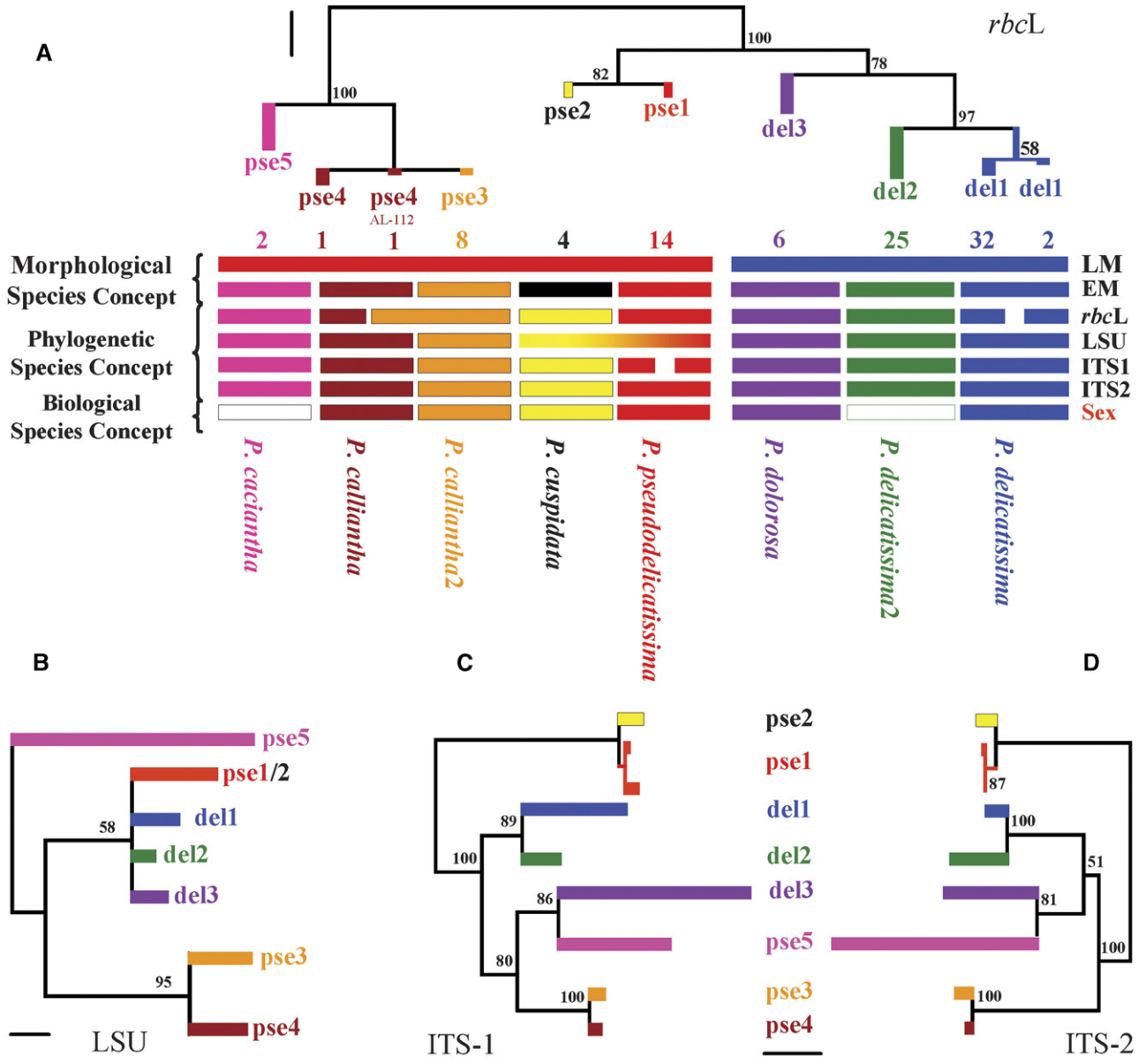

Figure 2. ML tree inferred from *rbc*L **(A)**, LSU **(B)**, ITS-1 **(C)**, and ITS-2 **(D)** sequences. Boldface numbers in each node indicate the bootstrap values (1000 replicates). **(A)** Numbers in the first row represent the number of strains analysed. Horizontal bars indicate the clustering patterns recognized by gross (LM) and ultrastructural (TEM) morphology, molecular markers (listed on the right side), and sexual compatibility. The black solid rectangle indicates that ultrastructural analyses were not carried out, the green empty rectangle that mating experiments were performed (see text and Table 2) but never produced sexual stages, and black empty rectangle that mating experiments were not performed. Scale bars: 0.01 **(A)**, 0.005 **(B)**, and 0.05 substitutions/site **(C,D)**.

organization of poroids into biseriate striae, (i.e. striae consisting of two rows of poroids; see Fig. 1D); however, they differed significantly in the densities of the striae and fibulae ($p << 0.001$) as well as in cell width and poroid density ($p < 0.05$) (Table 1).

The *P. pseudodelicatissima*-like strains grouped into five morphologically and ultrastructurally distinct groups. One of them (pse1, red) corresponded to *P. pseudodelicatissima sensu stricto*, another (pse4, dark brown) to *P. calliantha*,

Table 1. Morphometric data (valvar width, number of fibulae, and striae in 10 μm, number of poroids in 1 μm, number of sectors in the poroid) for *Pseudo-nitzschia* clades, together with published data on the corresponding described species (identities in parenthesis), where possible. The genotype codes correspond to those used in Figure 2.

	Valvar width (μm)	Fibulae/10 μm	Striae/10 μm	Poroids/1 μm			Poroid sectors
del1 (*Pseudo-nitzschia delicatissima*)							
Range	1.8—2.3	21—26	38—41	6—10			—
Average (s.d.)	2.0 (0.14)	23.1 (1.07)	39.1 (0.70)	7.8 (0.84)			—
N	50	64	64	229			—
(Amato et al. 2005)	≅2	22—29	33—43	8—11			—
(Lundholm et al. 2006)	1.4—2.1	18—26	34—41	8—12			—
del2 (*Pseudo-nitzschia delicatissima*2)							
Range	1.5—1.8	23—28	42—44	7—10			—
Average (s.d.)	1.6 (0.10)	25.0 (1.31)	42.8 (0.57)	7.9 (0.75)			—
N	74	60	58	180			—
del3 (*Pseudo-nitzschia dolorosa*)							
Range	2.7—3.8	18—25	33—43	5—11	5—8[a]	6—11[b]	—
Average (s.d.)	3.2 (0.22)	21.5 (1.67)	37.6 (2.35)	6.9 (1.24)	6.4[a] (0.84)	8.1[a] (1.04)	—
N	32	31	33	266	163[a]	103[a]	—
(Lundholm et al. 2006)	2.5—3.0	18—22	30—36	5—8			
pse1 (*Pseudo-nitzschia pseudodelicatissima*)							
Range	1.5—1.9	20—29	34—45	4—7			
Average (s.d.)	1.8 (0.13)	23.5 (1.83)	41.8 (1.87)	5.6 (0.59)			
N	41	45	50	262			
(Lundholm et al. 2003)	1.1—1.4	20—28	36—42	5—6			2
pse3 (*Pseudo-nitzschia calliantha*2)							
Range	1.7—2.6	17—25	30—40	4—6			2—7
Average (s.d.)	2.1 (0.24)	20.2 (1.95)	35.8 (2.06)	4.8 (0.31)			3.5 (0.97)
N	23	26	31	173			379
pse4 (*Pseudo-nitzschia calliantha*)							
Range	1.7—2.4	18—24	32—39	4—6			3—10
Average (s.d.)	2.1 (0.22)	19.7 (1.40)	36.8 (1.68)	4.7 (0.41)			5.6 (1.35)
n	32	32	32	229			428
(Lundholm et al. 2003)	1.4—1.8	17—21	34—39	4—6			Several
pse5 (*Pseudo-nitzschia caciantha*)							
Range	2.2—3.0	18—23	33—37	3—5			2—6
Average (s.d.)	2.6 (0.23)	20.7 (1.46)	34.9 (1.48)	4.6 (0.14)			3.1 (0.97)
N	8	9	7	55			220
(Lundholm et al. 2003)	2.7—3.5	15—19	28—31	3.5—5			4

[a]Number of poroids in the uniseriate striae in *Pseudo-nitzschia dolorosa.*
[b]Number of poroids in the biseriate striae in *Pseudo-nitzschia dolorosa*.

and a third (pse5, pink) to *P. caciantha* (Lundholm et al. 2003). A fourth group of strains (pse3, orange) was morphologically similar to *P. calliantha* (pse4) and the densities of their fibulae and striae were not significantly different ($p > 0.1$). However, the number of sectors within the poroids (5.6 in pse3 vs. 3.5 in pse4, Table 1) and the percentage of poroids possessing a central sector (2.1% in pse3 vs. 40.7% in pse4, Table 1) were significantly different ($p << 0.001$) between the two groups of strains. We were unable to examine the ultrastructure of strains pse2 (marked yellow), but their ITS regions conformed to that of *P. cuspidata* (Lundholm et al. 2003).

Mating Experiments and Sexual Compatibility

Progressive size reduction was observed in all groups, indicating that auxospore formation — and hence probably a sexual phase — is required to restore maximum cell size. However, mating among strains del2 invariably failed, notwithstanding our substantial efforts to find the right triggers

(723 attempts, testing temperature and day-length settings matching those recorded in the Gulf of Naples during different seasons, see Table 2). It seems unlikely that the 25 strains belonged to the same mating type because they were isolated from net samples collected on different dates (Table 3). In all other genotypes, the mating-type ratio was close to 1:1, and even among small numbers of isolates, opposite mating types were always recorded. Many diatoms have relatively narrow size windows for sexualization, but in del2, we failed to obtain any sexual reproduction among cells between 62 and 15 μm in length.

All groups within which sexual reproduction was successful showed a heterothallic mating system; homothally — sexual reproduction within a clonal culture — was never observed. Features of the sexual cycle matched those described for *P. delicatissima* (del1) (Amato et al. 2005). Mating experiments were carried out to verify sexual compatibility within genotypic groups and to assess mating boundaries amongst them (Fig. 2A, Table 2). Successful crosses were defined as those in which auxospores produced enlarged initial cells capable of dividing, giving rise within a few days to short chains of F1 cells. Successful crosses were restricted to crosses made within ITS-2 clades. Interclade crosses between strains belonging to pse3 and pse4 (including strain AL-112, the one with nuclear genotype pse4 but *rbc*L haplotype pse3) led to successful pairing of gametangia and conjugation of gametes, but the resulting zygotes never developed into auxospores.

ITS-2 Secondary Structure

To identify genetic characteristics at the species level and below, we compared the secondary structure of ITS-2 rDNA sequences for all genotypes and determined the Compensatory Base Changes (CBC including Hemi-CBC [HCBC], changes on one side only) according to Coleman (2000, 2003). Results of the comparisons are provided in Figure 3. The secondary structures of all strains had the same organization with four helices (I, II, III, and IV); an additional helix (IIa), which is characteristic for *Pseudo-nitzschia* and some other diatoms, was identified between helices II and III. The ITS-2 rDNA sequences differed in length and in the composition of the end-loops in the helices (Fig. 3). The conserved regions of ITS-2 are highlighted in boldface in Figure 3. The closely related *P. pseudodelicatissima*

Table 2. Matrix of crosses. Number of crosses performed within and among the different genotypes identified basing on the ITS-2 clades (see Fig. 2). Grey boxes = successful sexual reproduction observed; white boxes = sexual reproduction not observed; black boxes = combination not tested.

Genotypes:	del1	del2	del3	pse1	pse2	pse3	pse4
No. of tested strains	34	25	5	17	4	2	8
del1	392	133	10	118	8	4	10
del2		723	16	52	–	12	16
del3			29	72	10	–	2
pse1				118	31	4	12
pse2					–	–	–
pse3						19	17
pse4							41

Table 3. Strains analysed in the present study; strain code, LSU, ITS rDNA and *rbc*L GenBank accession numbers (in boldface), and date of isolation are reported. Species names and genotype code correspond to those listed in Figure 2.

Strain code	LSU accession #	ITS accession #	*rbc*L accession #	Isolation date
del1 (*Pseudo-nitzschia delicatissima* (Cleve) Heiden)				
18-02[a]	**AY519349**	**AY519334**	As AL-24	27 Mar 02
24-02[a]	**AY519351**	**AY519335**	As AL-24	27 Mar 02
26-02[a]	**AY519352**	**AY519337**	As AL-24	27 Mar 02
27-02 [a]	**AY519353**	**AY519336**	As AL-24	27 Mar 02
AL-18	As AL-24	—	As AL-24	21 Jan 04
AL-23	As AL-24	As AL-24	As AL-24	21 Jan 04
AL-24	**DQ813811**	**DQ813830**	**DQ813819**	21 Jan 04
AL-47	As AL-24	—	As AL-24	02 Feb 04
AL-63	As AL-24	—	As AL-24	05 Feb 04
AL-64	As AL-24	As AL-24	**DQ813823**	05 Feb 04
AL-65	As AL-24	—	As AL-24	09 Feb 04
AL-73	As AL-24	—	As AL-24	16 Feb 04
AL-79	As AL-24	As AL-24	As AL-24	05 Apr 04
AL-81	As AL-24	—	As AL-24	05 Apr 04
AL-82	As AL-24	—	As AL-24	05 Apr 04
AL-83	As AL-24	—	As AL-24	05 Apr 04
AL-85	As AL-24	—	—	05 Apr 04
AL-86	As AL-24	—	—	31 Mar 04
AL-88	As AL-24	As AL-24	As AL-64	16 Apr 04
AL-90	As AL-24	—	As AL-24	22 Apr 04
AL-91	As AL-24	—	As AL-24	22 Apr 04
S-AL-4[b,c]	As AL-24	—	—	—
AL-103	As AL-24	—	As AL-24	15 Mar 05
AL-105	As AL-24	As AL-24	As AL-24	15 Mar 05
AL-106	As AL-24	—	As AL-24	15 Mar 05
AL-107	As AL-24	—	As AL-24	15 Mar 05
AL-109	As AL-24	—	As AL-24	15 Mar 05
AL-110	As AL-24	**DQ813840**	As AL-24	15 Mar 05
AL-111	As AL-24	As AL-24	As AL-24	15 Mar 05
AL-113	As AL-24	—	As AL-24	15 Mar 05
AL-116	As AL-24	As AL-24	As AL-24	15 Mar 05
AL-118	As AL-24	—	As AL-24	15 Mar 05
AL-119	—	—	As AL-24	15 Mar 05
AL-120	As AL-24	As AL-24	As AL-24	15 Mar 05
del2 (*Pseudo-nitzschia delicatissima2*)				
21-02[a]	**AY519350**	**AY519281**	—	27 Mar 02
AL-22	**DQ813810**	**DQ813829**	**DQ813818**	21 Jan 04
AL-34	As AL-22	—	As AL-22	21 Jan 04
AL-36	As AL-22	As AL-22	As AL-22	21 Jan 04
AL-38	As AL-22	**DQ813832**	As AL-22	21 Jan 04
AL-51	As AL-22	As AL-22	As AL-22	02 Feb 04
AL-55	As AL-22	As AL-22	As AL-22	02 Feb 04
AL-62	As AL-22	As AL-22	As AL-22	05 Feb 04
AL-70	As AL-22	As AL-22	As AL-22	05 Feb 04
AL-71	As AL-22	—	As AL-22	05 Feb 04
AL-72	As AL-22	As AL-22	As AL-22	05 Feb 04
AL-80	As AL-22	As AL-22	As AL-22	05 Apr 04
AL-87	As AL-22	As AL-22	As AL-22	05 Apr 04
AL-89	As AL-22	As AL-22	As AL-22	22 Apr 04
S-AL-1[b]	As AL-22	**DQ813843**	As AL-22	—

Table 3. (*continued*)

Strain code	LSU accession #	ITS accession #	*rbc*L accession #	Isolation date
S-AL-2[b]	As AL-22	—	As AL-22	—
AL-94	As AL-22	As AL-22	As AL-22	18 Jun 04
AL-95	As AL-22	—	As AL-22	18 Jun 04
AL-95bis	As AL-22	As AL-22	As AL-22	18 Jun 04
AL-95ter	As AL-22	As AL-22	As AL-22	18 Jun 04
AL-96	As AL-22	As AL-22	As AL-22	18 Jun 04
AL-97	As AL-22	As AL-22	As AL-22	18 Jun 04
AL-97bis	As AL-22	As AL-22	As AL-22	18 Jun 04
AL-97ter	As AL-22	As AL-22	As AL-22	18 Jun 04
AL-97quater	As AL-22	—	—	18 Jun 04
del3 (*Pseudo-nitzschia dolorosa* Lundholm et Moestrup)				
20-02[a]	**AY519348**	**AY519275**	—	27 Mar 02
AL-59	**DQ813813**	**DQ813835**	**DQ813822**	02 Feb 04
AL-67	As AL-59	**DQ813837**	As AL-59	05 Feb 04
AL-69	—	—	As AL-59	05 Feb 04
AL-74	As AL-59	**DQ813838**	As AL-59	16 Feb 04
C-AL-2[c]	As AL-59	As AL-59	As AL-59	25 Feb 04
pse1 (*Pseudo-nitzschia pseudodelicatissima* (Hasle) Hasle emend. Lundholm, Hasle et Moestrup)				
SZN-B109[a]	**AY550126**	As AL-41	—	04 Jun 02
SZN-B111[a]	**AY550128**	As AL-41	—	04 Jun 02
SZN-B112[a]	**AY550127**	—	—	04 Jun 02
SZN-B113[a]	**AY550129**	—	—	04 Jun 02
AL-15	**DQ813808**	**DQ813826**	**DQ813817**	19 Jan 04
AL-19	As AL-15	**DQ813828**	As AL-15	21 Jan 04
AL-20	As AL-15	As AL-19	As AL-15	21 Jan 04
AL-21	As AL-15	As AL-41	As AL-15	21 Jan 04
AL-27	As AL-15	As AL-19	As AL-15	26 Jan 04
AL-29	As AL-15	**DQ813831**	—	26 Jan 04
AL-31	As AL-15	—	—	26 Jan 04
AL-40	As AL-15	As AL-19	As AL-15	02 Feb 04
AL-41	As AL-15	**DQ813833**	As AL-15	02 Feb 04
AL-60	As AL-15	**DQ813836**	As AL-15	02 Feb 04
pse2 (*Pseudo-nitzschia cuspidata* (Hasle) Hasle emend. Lundholm, Moestrup et Hasle)				
AL-17	**DQ813809**	**DQ813827**	—	19 Jan 04
AL-28	As AL-15	As AL-17	**DQ813820**	26 Jan 04
AL-57	As AL-15	As AL-17	As AL-28	02 Feb 04
AL-61	As AL-15	As AL-17	As AL-28	02 Feb 04
pse3 (*Pseudo-nitzschia calliantha* 2)				
P2[a]	As AL-101	—	—	17 Jan 02
P4[a]	**DQ813816**	—	—	17 Jan 02
P5[a]	As AL-101	As AL-101	—	17 Jan 02
P6[a]	—	As AL-101	—	17 Jan 02
AL-11	As AL-101	—	As AL-101	07 Oct 03
AL-13	As AL-101	—	As AL-101	07 Oct 03
AL-101	**DQ813814**	**DQ813839**	**DQ813824**	14 Oct 04
C-AL-1[c]	As AL-101	**DQ813842**	As AL-101	25 Feb 04
pse4 (*Pseudo-nitzschia calliantha* Lundholm, Moestrup et Hasle)				
AL-112	**DQ813815**	**DQ813841**	As AL-101	15 Mar 05
AL-117	As AL-112	As AL-112	**DQ813825**	15 Mar 05

Table 3. (*continued*)

Strain code	LSU accession #	ITS accession #	*rbc*L accession #	Isolation date
pse5 (*Pseudo-nitzschia caciantha* Lundholm, Moestrup et Hasle)				
AL-46[c]	As AL-56	—	As AL-56	26 Jan 04
AL-56[c]	**DQ813812**	**DQ813834**	**DQ813821**	02 Feb 04

[a]Strain isolated by Luisa Orsini.
[b]Strain isolated by Sarah M. McDonald.
[c]Strain not used in crossing experiments: — = information not available.

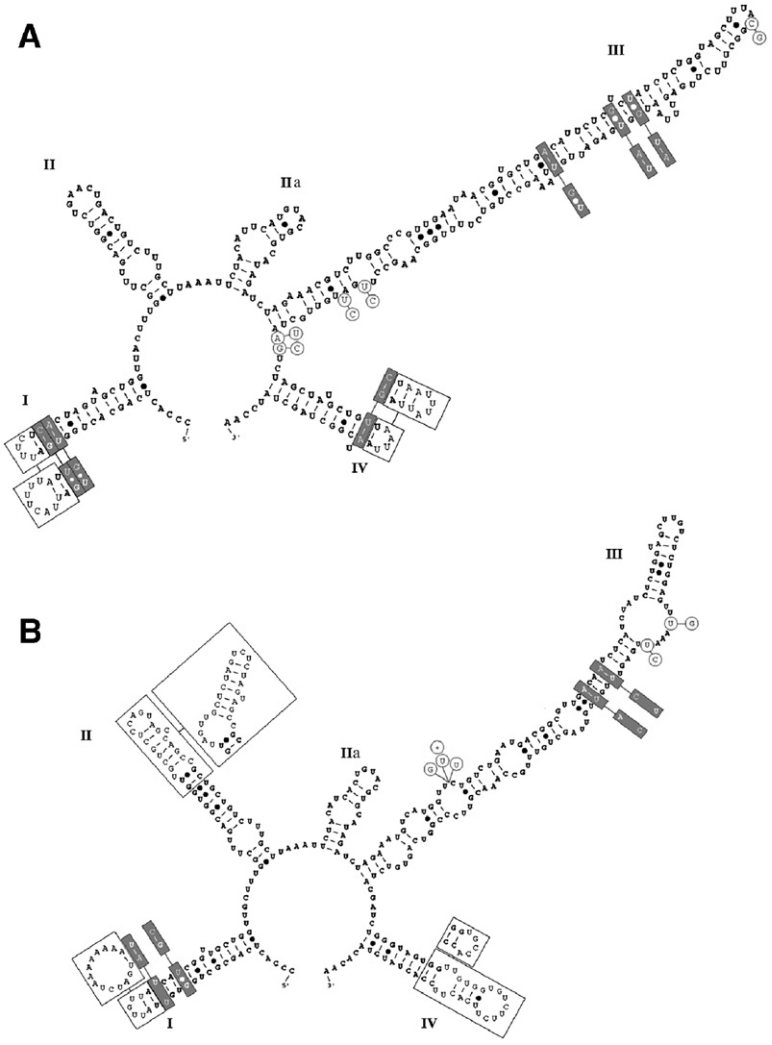

Figure 3. ITS-2 rRNA secondary structure models of **(A)** *Pseudo-nitzschia pseudodelicatissima* (strain AL-15; pse1) and **(B)** *Pseudo-nitzschia calliantha* (strain AL-112; pse4). The base pairs marked in grey indicate compensatory base changes (CBC or HCBC) compared to strains AL-17 (pse2) in **(A)** and AL-101 (pse3) in **(B)**. In circles are marked single base changes and in boxes the changes of the ends in the helices between the strains respectively. The conserved regions of ITS-2 are highlighted in bold.

(pse1) and *P. cuspidata* (pse2) (Fig. 3A) differed in two HCBCs (marked in grey in Fig. 3A) occurring in helix I (**U**:A ↔ **U**:G and **G**:C ↔ **G**:U), three in helix III (A:**U** ↔ G:**U**, G:**U** ↔ A:**U**, and **U**:G ↔ **U**:A), and one CBC in helix IV (U:A ↔ C:G). In *P. calliantha* (pse4) and *P. calliantha*2 (pse3) (Fig. 3B), two

HCBCs (marked in grey in Fig. 3B) were recorded in helix I, **G**:U ↔ **G**:C, U:**U** ↔ A:**U**; the latter involving a non-canonical but proven pair (Gutell 1994). Two base changes that break two bonds, A:U ↔ A C and A:U ↔ C U, were recorded in helix III; the latter could produce the non-canonical pair Y:Y (Gutell 1994).

Discussion

Our data show that groups of *Pseudo-nitzschia* strains distinguished on the basis of four molecular markers are reproductively isolated. Since all these genetically distinct groups occur in sympatry in the Gulf of Naples, they must constitute biologically distinct species. Genetically and biologically distinct species within the *P. delicatissima*-like group reveal subtle ultrastructural differences, and the same applies for those within the *P. pseudodelicatissima*-like group. However, identification is extremely difficult and the ranges of morphometric examined characters often overlap. Thus, species within each of these groups can be defined as pseudo-cryptic (semi-cryptic *sensu* Mann 1999) species.

We tested genetic relatedness among the different strains using three nuclear and one plastid marker that are widely used in assessing relationships at the species level or below (Lundholm et al. 2003; Paul et al. 2000; Sarno et al. 2005). Of these four markers, ITS-2 appears to be the only one that discriminates accurately between biological species. Two strains mated successfully only if they had ITS-2 sequences with identical helix regions. The LSU region is not a perfect discriminator because in one case, this region did not separate two different species (pse1 and pse2 = *P. pseudodelicatissima* and *P. cuspidata*) that failed to interbreed and possessed different *rbc*L and ITS sequences. The *rbc*L marker is not a perfect discriminator either, because pairs of *P. delicatissima* (del1) strains with different *rbc*L genotypes mated successfully, i.e. they generated a perfectly viable and fertile F1 generation. These two groups of strains possessed identical LSU and ITS sequences. Apparently, different *rbc*L haplotypes can occur within a single interbreeding population. ITS-1 is also unsatisfactory as a biological species discriminator, because compatible *P. pseudodelicatissima* (pse1) strains generate a viable F1 generation, irrespective of their ITS-1 genotype.

Phylogenetic trees based on ribosomal and chloroplast markers show minor differences in the ramifications, but they generally corroborate one another in the grouping of sequences in end nodes. There are four deviations from this concordance. (1) Single interbreeding species *P. delicatissima* (del1) possesses two *rbc*L types. The polymorphism may be recent or ancient (Takahashi et al. 2001) and may have arisen before or after separation of del1 from other lineages. It is possible that one of the variants was introduced by hybridization with some other unknown 'del' lineage. (2) Within *P. calliantha*, strain AL-112 has the *rbc*L haplotype of pse3, but shares the LSU and ITS genotypes with pse4. It also has the ultrastructure of pse4 and interbreeds successfully with the compatible strain of pse4, but not with the ones of pse3. Again, it is possible that this pattern arose through introgression, followed by repeated backcrossing of the hybrid offspring with *P. calliantha* pse4. (3) The different ITS-1 sequences found in *P. pseudodelicatissima* (pse1) could be interpreted as a case of polymorphism not yet homogenized by concerted evolution, and the region in which it occurs could be a fast-evolving one. Anyway, the strains share identical sequences at all other markers investigated and interbreed freely. (4) The shared LSU genotype of *P. pseudodelicatissima* (pse1, red) and *P. cuspidata* (pse2, yellow) is probably because the LSU region generally evolves more slowly than the ITS regions. The other markers indicate that the two taxa are close relatives, suggesting that the LSU marker has not had enough time to accumulate differences.

Although ITS-1 and ITS-2 are transcribed regions but are not part of the mature ribosomes, they have complex secondary structures and play a crucial role in the construction of ribosomes (Tschochner and Hurt 2003). Thus, the sequences corresponding to the helix regions are functionally constrained and only those few base changes that do not interfere with the proper folding of the primary transcripts (CBCs or HCBCs) are permissible (Gutell 1994). The secondary structures of the ITS-2 region in *Pseudo-nitzschia* species analysed in the present study show the distinct eukaryotic hallmarks: (1) four main helices, (2) of which helix III is the longest, (3) the presence of a characteristic motif at the apex of helix III, and (4) a pyrimidine-pyrimidine mismatch in helix II (Schultz et al. 2005). A correlation between ITS-2 sequence evolution and sexual compatibility was shown for green freshwater microalgae of the order Volvocales (Chlorophyta) and for the ciliate *Paramecium aurelia* (Coleman 2000, 2005; Fabry et al. 1999). Reproductive isolation occurred if

there were CBCs or HCBCs, but the reverse was not necessarily true: some pairs of *Paramecium* syngens were effectively reproductively isolated, despite having identical ITS sequences. The *Pseudo-nitzschia* ITS-2 genotypes analysed in the present study belong to different CBC-clades and do not show any sexual interactions with each other. The only exception concerns pse4 (*P. calliantha*) and pse3, whose ITS-2 differed by three HCBCs but where the gametangia still recognized one another as potential mates and gametes fused into a zygote. However, that is where the process stopped; the zygote failed to develop into an auxospore. The most closely related species grouping in different CBC-clades were *P. pseudodelicatissima* (pse1) and *P. cuspidata* (pse2). In fact, they differ by only one CBC (and five HCBCs) and their cells did not even recognize one another as potential partners. This finding confirms that strains clustering in different CBC-clades are sexually incompatible.

ITS-2 secondary structures are available for only very few microalgae; nevertheless, these few results already reveal that the number of CBCs (including HCBCs) at which reproductive isolation sets in differs among phylogenetic groups. Mating compatibility among strains of the chlorophycean *Gonium pectorale* is compromised if they differ by even one HCBC in conserved helix regions (Coleman 2000). Behnke et al. (2004) found variations in ITS rDNA sequences between locally interbreeding populations of the benthic freshwater diatom *Sellaphora pupula*. However, the secondary structure of ITS-2 is unique for *Sellaphora* and is not comparable to that of other diatoms and eukaryotes.

Few studies have evaluated the capacity of morphological and molecular data to resolve relationships among species of marine planktonic protists, and even fewer have provided matching information about reproductive isolation. Molecular data revealed genetic differentiation among morphologically apparently identical planktonic foraminifera, but subsequent morphological investigations revealed small differences in the porosity of the calcareous test (de Vargas et al. 1999; Huber et al. 1997). Also in coccolithophorids, different genotypes match differences in cell and coccolith size and morphology (Sáez et al. 2003). All *Pseudo-nitzschia* strains examined in our study share the same gross morphology, suggesting that their cell shape and colony type are adaptations for life in the planktonic environment. The fact that reproductively isolated, genetically differentiated *Pseudo-nitzschia* species also show small but consistent ultrastructural differences in their frustule architecture, which has been the principal trait for their taxonomy since 1965 (Hasle 1965; Hasle et al. 1996), suggests that these morphological differences are ecologically relevant as well. The stria pores, occluded by sieve-like membranes (hymenes) serve as transport channels between the exterior environment and the cytoplasm and it has been shown that they might control diffusion and advection of particles and molecules, acting as particle sorters (Hale and Mitchell 2001; Losic et al. 2006). Kumar (1980) showed that they can also be the points of entry for species-specific parasitoids (although the raphe is another and larger potential route for infection in *Pseudo-nitzschia*) and, potentially, for viruses. Many algal species, including *Pseudo-nitzschia* (Elbrächter and Schnepf 1998; Rosowski et al. 1992), are proving to be affected by parasites and the highly species-specific host—parasite interaction characterized by continuous reciprocal selection, might result in rapid co-evolution with a corresponding diversification of the ultrastructure of the host organism (cf. Mann 1999, p. 481).

The finding of reproductive isolation among *Pseudo-nitzschia* strains that are genetically distinct but morphologically nearly identical raises questions about the ecological meaning of this hidden diversity. Classical ecological competition theory predicts that species, including cryptic species, can coexist at equilibrium only if they show some level of ecological specialization (Hutchinson 1978; Tilman 2004). Although our understanding of the biological characteristics of marine plankton is rather limited, there are data supporting the idea that different cryptic species occupy distinct ecological niches. For example, among planktonic foraminifera, the large-scale spatial distribution of different genotypes of *Orbulina universa* is correlated with hydrographic province and surface ocean primary production (de Vargas et al. 1999) and such variation can have important consequences for reconstruction of past oceanographic conditions (Kucera and Darling 2002). In a study carried out during a spring bloom of *P. delicatissima* in the Gulf of Naples, three '*delicatissima*' ITS types (corresponding to del1, del2, and del3 of the present study) were recorded together in pre-bloom conditions, but only one of them (del1) contributed substantially to the spring bloom (Orsini et al. 2004). The partition of distinct genotypes between different temporal windows — i.e. blooming at different times while maintaining a low concentration all year round — in an annual or multi-annual cycle might represent

a strategy for sharing the same environment. As an example, different populations of *Skeletonema costatum* characterized by distinct isozyme banding patterns — possibly pseudo-cryptic species (Sarno et al. 2005) — were recorded during the spring and autumn blooms in Narragansett Bay (Gallagher 1980). An additional clue that cryptic species behave differently comes from our failure to entice the strains of the del2 genotype to mate. Whatever the explanation for the lack of sexual reproduction in culture, this genotype clearly has peculiar life cycle traits or requirements for sexual induction as compared to closely related genotypes. Cryptic diversity may explain the observed strain-specific differences in the capacity for producing toxins (Mos 2001) or secondary metabolites (Wichard et al. 2005), which may confer selective advantages to particular genotypes.

The finding of cryptic or pseudo-cryptic diversity will be 'annoying' for ecologists who identify and enumerate phytoplankton using light microscopy. We are in fact confronted with the impossibility of recognizing the units of interest — species — with standard tools. However, a level of complexity higher than has previously been realized may provide the key for interpreting apparently meaningless patterns in the distribution, biology, and succession of phytoplankton species.

It is remarkable that by sampling 95 strains of *P. delicatissima*- and *P. pseudodelicatissima*-like diatoms at a single site we uncovered all but one (*P. decipiens*) of the genotypes previously described for these species complexes on the basis of strains isolated from a series of geographically distant localities (Lundholm et al. 2003, 2006). Moreover, we found two novel genotypes, showing that genetic diversity within the two species complexes is probably even wider. The existence of closely related but genetically distinct populations living in sympatry implies the evolution of effective mechanisms of reproductive isolation that prevent interbreeding and we have demonstrated these by direct tests of compatibility. During bloom conditions — in which cell concentrations increase greatly — encounter rates among gametangia will be maximal. Thus, if the timing of the bloom differs among different genotypes, the chances of finding conspecific cells within the bloom will be high and may largely or completely prevent interbreeding. If, on the other hand, blooms are mixed, then efficient recognition systems should evolve, allowing discrimination between members of the same species and others. Our data indicate a lack of prezygotic isolation only between pse3 and pse4, indicating that there has usually been selection for efficient recognition. The genetic composition of blooms awaits more detailed study and is crucial for elucidating the mode of speciation in these *Pseudo-nitzschia* species, which represent a valuable model system for investigating the evolution of marine phytoplankton.

Methods

Cultures and Mating Experiments: Strains analysed in the present work are listed in Table 3. Selected strains were prepared for electron microscopy as described in Orsini et al. (2004) and examined with a TEM LEO 912AB or a SEM JEOL JSM-6500F (JEOL-USA Inc., Peabody, MA, USA). The following ultrastructural characters of the frustule used in morpho-taxonomy (Lundholm et al. 2003, 2006) were estimated: (1) valve width, (2) number of fibulae (Fig. 1C,D; dotted arrows) in 10 μm, (3) number of striae (Fig. 1C,D; solid ellipses) in 10 μm, (4) the number of poroids (Fig. 1C,D; arrowheads) in 1μm, and (5) the number of sectors in the poroids. The statistical significance of morphometric differences among the different genotypes was tested with Student's *t*-test.

Mating experiments were carried out by mixing pairs of exponentially growing cultures at concentrations of about 4000 cells ml^{-1} for each strain and incubating them at 18 °C, 100 μmol photons m^{-2} s^{-1}, and 14:10 h L:D photocycle. Controls were run with the single strains, and a compatible pair of *P. delicatissima* (del1) strains was used as positive control. Before performing the experiments, cell length was measured using LM. For del2 strains, additional mating experiments were run at higher (150 μmol photons m^{-2} s^{-1}) and lower (10 μmol photons m^{-2} s^{-1}) irradiances, and with cell concentrations of 2000 and 8000 cells ml^{-1}. With these strains, experiments were also run at different daylengths and temperatures, simulating those recorded in summer (23 °C and 14:10 h L:D), early autumn (23 °C and 12:12 h L:D), and late autumn (18 °C and 9:15 h L:D) in the Gulf of Naples.

DNA Analyses: Genomic DNA was extracted following Kooistra et al. (2003), then amplified by polymerase chain reaction (PCR) using the primers D1R and D3Ca (Lenaers et al. 1989; Scholin et al. 1994) for the hypervariable domains 'D1' and 'D3'of LSU rDNA, and using the universal primers ITS1 and ITS4 (White et al. 1990) for the ITS rDNA regions. Forty cycles (35 s at 94 °C, 35 s at 46.2 °C, and 60 s at 72 °C) were performed, with an initial

step of 120 s at 94 °C and a final one of 300 s at 72 °C. The *rbc*L region was amplified using the two degenerated primers modified from DP*rbc*L1 and DP*rbc*L7 (Daugbjerg and Andersen 1997). Thirty-five cycles (60 s at 94 °C, 60 s at 55 °C, and 90 s at 72 °C) were performed, with an initial step of 180 s at 94 °C, and a final one of 300 s at 72 °C.

Ribosomal fragments were directly sequenced using the amplification primers, while *rbc*L fragments were sequenced using amplification primers as external sequence primers and two internal primers, *rbc*L I1F (5'-TTAGAAGACATGCGTATT) modified from 16F (Jones et al. 2005) and *rbc*L I1R (5'-CAGTGTAACCCATAAC) modified from ND*rbc*L11 (Daugbjerg and Andersen 1997). Sequence reactions were obtained with the BigDye Terminator Cycle Sequencing technology (Applied Biosyhelixs, Foster City CA) and purified in automation using the robotic station Biomek FX (Beckman Coulter, Fullerton CA). Products were analysed on an Automated Capillary Electrophoresis Sequencer 3730 DNA Analyzer (Applied Biosyhelixs). Sequences were assembled using the SeqMan II 3.61 computer program (DNASTAR inc.) and then aligned using ClustalW (Thompson et al. 1994) in BioEdit 7.01 (Hall 1999). Distance (neighbor-joining; NJ) and maximum likelihood (ML) analyses were conducted using MEGA 3.0 (Kumar et al. 2004) and PAUP* version 4.0b10 (Swofford 2002). ML analysis of *rbc*L sequences (Fig. 2A) considered 1st, 2nd, and 3rd codon positions and was constrained with GTR+I (Modeltest 3.06, Posada and Crandall 1998; AIC, Akaike 1974); resulting tree-length: 151 steps; rescaled consistency index: 0.758; homoplasy index: 0.159. The ML tree inferred from LSU (Fig. 2B) was obtained with likelihood settings from best-fit model GTR+I (Modeltest 3.06; AIC). The NJ trees based on ITS-1 and ITS-2 (Fig. 2C, D) were inferred from pairwise Kimura-2-parameter distances. Confidence of branching was assessed using 1000 bootstrap replicates and the same settings as in the NJ or ML analyses.

The secondary structures of ITS-2 rDNA sequences were constructed using the mfold computer program (version 3.2; Mathews et al. 1999; Zuker 2003 http://www.bioinfo.rpi.edu/applications/mfold/rna/form1.cgi). The structures were summarized including the CBCs and HCBCs highlighted in Figure 3 using LoopDloop (version 2.02a; Gilbert 1992: http://iubio.bio.indiana.edu/soft/molbio/java/apps/loops/loopDloop-doc.html). The helices were then labelled according to Mai and Coleman (1997).

Acknowledgements

This work forms part of the Ph.D. programme of A.A. (Open University London, UK; Stazione Zoologica 'A. Dohrn', Napoli, Italy). The authors thank the Molecular Biology Service of the Stazione Zoologica 'A. Dohrn' for DNA sequencing; the Electron Microscopy service and G. Forlani for assistance in electron microscopy preparations. The project has been carried out in the frame of the MarBEF Network of Excellence 'Marine Biodiversity and Ecosystem Functioning' (contract no. GOCE-CT-2003-505446) and the Marine Genomics Europe Network of Excellence (contract no. GOCE-CT-2004-505403), which are funded in the EU's Sixth Framework Programme.

References

Akaike H (1974) A new look at the statistical model identification. IEEE Trans Contr **19**: 716—723

Amato A, Orsini L, D'Alelio D, Montresor M (2005) Life cycle, size reduction patterns, and ultrastructure of the pennate planktonic diatom *Pseudo-nitzschia delicatissima* (Bacillariophyceae). J Phycol **41**: 542—556

Behnke A, Friedl T, Chepurnov VA, Mann DG (2004) Reproductive compatibility and rDNA sequence analyses in the *Sellaphora pupula* species complex (Bacillariophyta). J Phycol **40**: 193—208

Chepurnov VA, Mann DG, Sabbe K, Vyverman W (2004) Experimental studies on sexual reproduction in diatoms. Int Rev Cytol **237**: 91—154

Coleman AW (2000) The significance of a coincidence between evolutionary landmarks found in mating affinity and a DNA sequence. Protist **151**: 1—9

Coleman AW (2003) ITS2 is a double-edged tool for eukaryote evolutionary comparisons. Trends Genet **19**: 370—375

Coleman AW (2005) *Paramecium aurelia* revisited. J Eukaryot Microbiol **52**: 68—77

Coyne JA, Orr HA (2004) Speciation. Sinauer Associates, Inc., Sunderland

Daugbjerg N, Andersen RA (1997) A molecular phylogeny of the heterokont algae based on analyses of chloroplast-encoded *rbc*L sequence data. J Phycol **33**: 1031—1041

Davidovich NA, Bates SS (1998) Sexual reproduction in the pennate diatoms *Pseudo-nitzschia multiseries* and *P. pseudodelicatissima* (Bacillariophyceae). J Phycol **34**: 126—137

de Vargas C, Norris R, Zaninetti L, Gibbs SW, Pawlowski J (1999) Molecular evidence of cryptic speciation in planktonic foraminifers and their relation to oceanic provinces. Proc Natl Acad Sci USA **96**: 2864—2868

Elbrächter M, Schnepf E. (1998) Parasites of Harmful Algae. In Anderson DM, Cembella AD, Hallegraeff GM (eds).

Physiological Ecology of Harmful Algae. Springer, Berlin, pp 350—369

Fabry S, Köhler A, Coleman AW (1999) Intraspecies analysis: comparison of ITS sequence data and gene intron sequence data with breeding data for a worldwide collection of *Gonium pectorale*. J Mol Evol **48**: 94—101

Fryxell GA, Garza SA, Roelke DL (1991) Auxospore formation in an Antarctic clone of *Nitzschia subcurvata* Hasle. Diatom Res **6**: 235—245

Gallagher JC (1980) Population genetics of *Skeletonema costatum* (Bacillariophyceae) in Narragansett Bay. J Phycol **16**: 464—474

Gilbert DG (1992) LoopDloop, a Macintosh program for visualizing RNA secondary structure, http://iubio.bio.indiana.edu/soft/molbio/java/apps/loops/loopDloop-doc.html

Guillou L, Eikrem W, Chrétiennot-Dinet MJ, Le Gall F, Massana R, Romari K, Pedròs- Aliò C, Valuot D (2004) Diversity of picoplanktonic prasinophytes assessed by direct nuclear SSU rDNA sequencing of environmental samples and novel isolates retrieved from oceanic and coastal marine ecosystems. Protist **155**: 193—214

Gutell RR (1994) Lessons from an evolving ribosomal-RNA - 16s and 23s ribosomal-RNA structures from a comparative perspective. Microbiol Rev **58**: 10—26

Hale MS, Mitchell JG (2001) Functional morphology of diatom frustule microstructures: hydrodynamic control of Brownian particle diffusion and advection. Aquat Microb Ecol **24**: 287—295

Hal TA (1999). BioEdit: A user-friendly biological sequence alignment editor and analysis program for Windows 95/98/NT. Nucleic Acids Symp Ser **41**: 95—98

Hasle GR (1965) *Nitzschia* and *Fragilariopsis* species studied in the light and electron microscopes. II. The group *Pseudo-nitzschia*. Skr Nor Vidensk-Akad Oslo I Mat-Naturvidensk Kl **18**: 1—45

Hasle GR, Syvertsen EE (1997) Marine Diatoms. In: Tomas CR (eds) Identifying Marine Phytoplankton. Academic Press, San Diego, pp 5—385

Hasle GR, Lange CB, Syvertsen EE (1996) A review of *Pseudo-nitzschia*, with special reference to the Skagerrak, North Atlantic, and adjacent waters. Helgol Meeresunters **50**: 131—175

Huber BT, Bijma J, Darling K (1997) Cryptic speciation in the living planktonic foraminifer *Globigerinella siphonifera* (d'Orbigny). Paleobiology **23**: 33—62

Hutchinson GE (1978) An Introduction to Population Ecology. Yale University Press, New Haven

Jones HM, Simpson GE, Stickle AJ, Mann DG (2005) Life history and systematics of *Petroneis* (Bacillariophyta), with special reference to British waters. Eur J Phycol **40**: 61—87

Knowlton N (1993) Sibling species in the sea. Annu Rev Ecol Syst **24**: 189—216

Kooistra WHCF, De Stefano M, Medlin LK, Mann DG (2003) The phylogenetic position of *Toxarium*, a pennate-like lineage within centric diatoms (Bacillariophyceae). J Phycol **39**: 185—197

Kucera M, Darling KF (2002) Cryptic species of planktonic foraminifera: their effect on palaeoceanographic reconstructions. Phil Trans R Soc Lond A **360**: 695—718

Kumar CR (1980) An ultrastructural study of the marine diatom *Licmophora hyalina* and its parasite *Ectrogella perforans*. I. Infection of host cells. Can J Bot **58**: 1280—1290

Kumar S, Tamura K, Nei M (2004) MEGA3: integrated software for molecular evolutionary genetics analysis and sequence alignment. Brief Bioinform **5**: 150—163

Lenaers G, Maroteaux L, Michot B, Herzog M (1989) Dinoflagellates in evolution. A molecular phylogenetic analysis of large subunit ribosomal RNA. J Mol Evol **29**: 40—51

Losic D, Rosengarten G, Mitchell JG, Voelcker NH (2006) Pore architecture of diatom frustules: Potential nanostructured membranes for molecular and particle separations. J Nanosci Nanotechnol **6**: 982—989

Lundholm N, Moestrup Ø, Hasle GR, Hoef-Emden K (2003) A study of the *Pseudo-nitzschia pseudodelicatissima/cuspidata* complex (Bacillariophyceae): what is *P. pseudodelicatissima*? J Phycol **39**: 797—813

Lundholm N, Moestrup Ø, Kotaki Y, Hoef-Emden K, Scholin C, Miller P (2006) Inter- and intraspecific variation of the *Pseudo-nitzschia delicatissima* complex (Bacillariophyceae) illustrated by rRNA probes, morphological data and phylogenetic analyses. J Phycol **42**: 464—481

Mai JC, Coleman AW (1997) The internal transcribed spacer 2 exhibits a common secondary structure in green algae and flowering plants. J Mol Evol **44**: 258—271

Mann DG (1999) The species concept in diatoms. Phycologia **38**: 437—495

Massana R, Castresana J, Balagué V, Guillou L, Romari K, Groisillier A, Valentin K, Pedròs-Aliò C (2004) Phylogenetic and ecological analysis of novel marine stramenopiles. Appl Environ Microbiol **70**: 3528—3534

Mathews DH, Sabina J, Zuker M, Turner DH (1999) Expanded sequence dependence of thermodynamic parameters improves prediction of RNA secondary structure. J Mol Biol **288**: 911—940

Montresor M, Sgrosso S, Procaccini G, Kooistra WHCF (2003) Intraspecific diversity in *Scrippsiella trochoidea* (Dinophyceae): evidence for cryptic species. Phycologia **42**: 56—70

Mos L (2001) Domoic acid: a fascinating marine toxin. Environ Toxicol Pharmacol **9**: 79—85

Orsini L, Procaccini G, Sarno D, Montresor M (2004) Multiple rDNA ITS-types within the diatom *Pseudo-nitzschia delicatissima* (Bacillariophyceae) and their relative abundances across a spring bloom in the Gulf of Naples. Mar Ecol Prog Ser **271**: 87—98

Paul JH, Alfreider A, Wawrik B (2000) Micro- and macrodiversity in *rbcL* sequences in ambient phytoplankton populations from the southeastern Gulf of Mexico. Mar Ecol Prog Ser **198**: 9—18

Posada D, Crandall KA (1998) Modeltest: testing the model of DNA substitution. Bioinformatics **14**: 818

Rosowski JR, Johnson LM, Mann DG (1992) On the report of gametogenesis, oogamy, and uniflagellated sperm in the pennate diatom *Nitzschia pungens*. J Phycol **28:** 570—574

Sáez AG, Lozano E (2005) Body doubles. Nature **433**: 111

Sáez AG, Probert I, Geisen M, Quinn P, Young JR, Medlin LK (2003) Pseudo-cryptic speciation in coccolithophores. Proc Natl Acad Sci USA **100**: 7163—7168

Sarno D, Kooistra WCHF, Medlin LK, Percopo I, Zingone A (2005) Diversity in the genus *Skeletonema* (Bacillariophyceae). II. An assessment of the taxonomy of *S. costatum*-like species, with the description of four new species. J Phycol **41**: 151—176

Scholin CA, Villac MC, Buck KR, Krupp JM, Powers DA, Fryxell GA, Chavez FP (1994) Ribosomal DNA sequences discriminate among toxic and non-toxic *Pseudonitzschia* species. Nat Toxins **2**: 152—165

Schultz J, Maisel S, Gerlach D, Müller T, Wolf M (2005) A common core of secondary structure of the internal transcribed spacer 2 (ITS2) throughout the Eukaryota. RNA-Publ RNA Soc **11**: 361—364

Swofford DL (2002) PAUP*-Phylogenetic Analysis Using Parsimony (* and other methods). Version 4.0b10. Sinauer Associates Inc, Sunderland, MA

Takahashi K, Terai Y, Nishida M, Okada N (2001) Phylogenetic relationships and ancient incomplete lineage sorting among cichlid fishes in Lake Tanganyika as revealed by analysis of the insertion of retroposons. Mol Biol Evol **18**: 2057—2066

Thompson JD, Higgins DG, Gibbson TJ (1994) Clustal W: improving the sensitivity of progressive multiple sequence alignment through sequence weighting, position-specific gap penalities and weight matrix choice. Nucleic Acids Res **22**: 4673—4680

Tilman D (2004) Niche tradeoffs, neutrality, and community structure: a stochastic theory of resource competition, invasion, and community assembly. Proc Natl Acad Sci USA **101**: 10854—10861

Tschochner H, Hurt E (2003) Pre-ribosomes on the road from the nucleolus to the cytoplasm. Trends Cell Biol **13**: 255—263

White TJ, Bruns T, Lee S, Taylor J (1990) Amplification and Direct Sequencing of Fungal Ribosomal RNA Genes for Phylogenetics. In Innis MA, Gelfand DH, Sninsky JJ, White TJ (eds) PCR Protocols. Academic Press, New York, pp 315—322

Wichard T, Poulet S, Halsband-Lenk C, Albaina A, Harris RP, Liu D, Pohnert G (2005) Survey of the chemical defence potential of diatoms: screening of fifty one species for a, b, c, d-unsaturated aldehydes. J Chem Ecol **31**: 949—958

Zuker M (2003) Mfold web server for nucleic acid folding and hybridization prediction. Nucleic Acids Res **31**: 3406—3415